Schematic model for QCD. II. Finite temperature regime

S. Jesgarz,[1,2,*] S. Lerma H.,[1,2,†] P. O. Hess,[1,‡] O. Civitarese,[2,§] and M. Reboiro[2,‖]
[1]*Instituto de Ciencias Nucleares, Universidad Nacional Autónoma de México, Apartado Postal 70-543, México 04510 D.F., Mexico*
[2]*Departamento de Física, Universidad Nacional de La Plata, c.c. 67 1900, La Plata, Argentina*
(Received 5 February 2003; published 30 May 2003)

A schematic model for QCD, developed in a previous paper, is applied to calculate meson properties in the high temperature (up to 0.5 GeV) regime. It is a Lipkin model for quark-antiquark pairs coupled to gluon pairs of spin zero. The partition function is constructed with the obtained meson spectrum and several thermodynamical observables are calculated, such as the energy density, heat capacity, as well as relative production rates of mesons and absolute production rates for pions and kaons. The model predictions show a qualitative agreement with data. Based on these results, we advocate the use of the model as a toy model for QCD.

DOI: 10.1103/PhysRevC.67.055210 PACS number(s): 12.90.+b, 21.90.+f

I. INTRODUCTION

In Ref. [1] [hereon referred to as (I)] a simple model, representative of QCD, was introduced and applied to the calculation of the spectrum of mesons. It is a Lipkin type model [2] for the quark sector, coupled to a boson level that is occupied by gluon pairs with spin zero. The four parameters of the model were adjusted in order to reproduce 13 known meson states with spin zero or one. The calculated spectra, for mesons with spin different from the ones used in the fit, were found to be in qualitative agreement with data. As reported in (I), the calculated meson states contain many quarks, antiquarks, and gluons. The gluon contributions were found to be of the order of 30%. The model predictions (I) are free of the so-called multiplicity problem, i.e., that a given state can be described in many ways, which is removed due to the action of particle mixing interaction. The model itself resembles the one of Ref. [3], which treats nucleons coupled to pions. Also, it is related to the work of Ref. [4], which describes quarks and uses particle conserving interactions. Generally speaking, the model of (I) belongs to the class of models described in Refs. [5,6]. The gluon part in (I) is fixed [7] and does not contain any new parameters. The validity of the basic theoretical assumptions, and the applications to low and high temperature regimes, has been studied for mesons with flavor (0,0) and spin 0 [8]. The aim of these studies was to formulate a manageable, schematic, albeit realistic, model to describe qualitatively QCD at low and high energies. Since the model is algebraic, i.e., all matrix elements are analytic, and exactly solvable, it can provide a nonperturbative description based on QCD relevant degrees of freedom, such as quarks, antiquarks, and gluons. This, in turn, allows to test other microscopic many body techniques previously applied to the nonperturbative treatment of real QCD [9,10]. Although the proposed model (I) is probably too simple to describe real QCD, it contains all basic ingredients of real QCD. These are the correct number of degrees of freedom associated with color, flavor, and spin, and the orbital degree of freedom, which is contained in the degeneracy 2Ω of each of the quark levels.

In this work we investigate the behavior of the model, in the finite temperature regime. By starting from the model predictions of the meson spectrum, we calculate the partition function and different thermodynamical quantities, such as the energy density and the heat capacity as a function of temperature. Next, we focus on the calculation of meson production rates. As we shall show, these production rates are in qualitative agreement with the experiments. Also, we calculate absolute production rates for pions and kaons. Finally, we concentrate on the transition from the quark-gluon-plasma (QGP) [11,12] to the hadron gas. The results support the notion that the present model may be taken as a toy model for QCD.

The paper is organized as follows: In Sec. II the model is shortly outlined, since the details have been presented in (I). In Sec. III we calculate the partition function and give the expressions for the relevant observables. In Sec. IV the model is applied to the description of the QGP. There, we present and discuss the results corresponding to some branching ratios and absolute production rates. Finally, conclusions are drawn in Sec. V.

II. THE MODEL

As described in (I), the fermion (quarks and antiquarks) sector of the model consists of two levels at energies $+\omega_f$ and $-\omega_f$, each level with degeneracy $2\Omega = n_c n_f n_s$, where $n_c = 3$, $n_f = 3$, and $n_s = 2$ are the color, flavor, and spin degrees of freedom, respectively [see Fig. 1 of (I)]. Each level can be occupied by quarks. Antiquarks are described by holes in the lower level. Equivalently, one can use only the positive energy level and fill it with quarks and antiquarks with positive energy. The Dirac picture is useful because it gives the connection to the Lipkin model as used in nuclear physics. The quarks and antiquarks are coupled to gluon pairs with spin zero. The energy of the gluon level is 1.6

*Email address: jesgarz@nuclecu.unam.mx
†Email address: alerma@nuclecu.unam.mx
‡Email address: hess@nuclecu.unam.mx
§Email address: civitare@fisica.unlp.edu.ar
‖Email address: reboiro@fisica.unlp.edu.ar

GeV [7], and the energy ω_f is fixed at the value $\omega_f = 0.33$ GeV, which is the effective mass of the constituent quarks.

The basic dynamical constituent blocks of the model are quark-antiquark pairs $\boldsymbol{B}^{\dagger}_{\lambda f,SM}$ that are obtained by the coupling of a quark and an antiquark to flavor λ ($\lambda=0,1$) and spin S ($S=0,1$). The index f is a shorthand notation for hypercharge Y, isospin I, and its third component I_z. Under complex conjugation the operator obeys the phase rule defined in Ref. [13].

The states of the Hilbert space can be classified according to the group chain

$$\begin{array}{lllll} [1^N] & [h]=[h_1h_2h_3] & & [h^t] \\ \mathrm{U}(4\Omega) & \supset \mathrm{U}\left(\dfrac{\Omega}{3}\right) & \otimes & \mathrm{U}(12) \\ & \cup & & \cup \\ (\lambda_C,\mu_C) & \mathrm{SU}_C(3) & (\lambda_f,\mu_f)\mathrm{SU}_f(3)\otimes\mathrm{SU}_S(2) & S,M, \end{array} \tag{1}$$

where the irreducible representations (irreps) of the different unitary groups are attached to the symbols of the groups. The irrep of $\mathrm{U}(4\Omega)$ is completely antisymmetric (fermions) and the ones of $\mathrm{U}(\Omega/3)$, the color group $\mathrm{U}(3)$ for $\Omega=9$, and $\mathrm{U}(12)$ are complementary [14]. The color irrep (λ_C,μ_C) of the color group $\mathrm{SU}_C(3)$ is related to the h_k via $\lambda_C=h_1-h_2$ and $\mu_C=h_2-h_3$. The reduction of the $\mathrm{U}(12)$ group to the flavor $[\mathrm{SU}_f(3)]$ and spin group $[\mathrm{SU}_S(2)]$ is obtained by using the procedure described in Refs. [15,16]. In Eq. (1) no multiplicity labels are indicated [see (I)].

The classification appearing in Eq. (1) is useful to determine the dimension and content of the Hilbert space. Instead of working in the fermion space we have introduced a boson mapping [17,18]. The quark-antiquark boson operators are mapped to

$$\boldsymbol{B}^{\dagger}_{\lambda f,SM}\rightarrow\boldsymbol{b}^{\dagger}_{\lambda f,SM},$$

$$\boldsymbol{B}_{\lambda f,SM}\rightarrow\boldsymbol{b}_{\lambda f,SM}, \tag{2}$$

where the operators on the right hand side satisfy exact boson commutation relations.

The model Hamiltonian is defined completely in the boson space and is given by

$$\begin{aligned}\boldsymbol{H}=&2\omega_f\boldsymbol{n}_f+\omega_b\mathbf{n}_{\mathbf{b}}+\sum_{\lambda S}V_{\lambda S}\Big\{[(\boldsymbol{b}^{\dagger}_{\lambda S})^2+2\boldsymbol{b}^{\dagger}_{\lambda S}\cdot\boldsymbol{b}_{\lambda S}+(\boldsymbol{b}_{\lambda S})^2]\\ &\times\left(1-\frac{\boldsymbol{n}_f}{2\Omega}\right)\boldsymbol{b}+\boldsymbol{b}^{\dagger}\left(1-\frac{\boldsymbol{n}_f}{2\Omega}\right)[(\boldsymbol{b}^{\dagger}_{\lambda S})^2+2\boldsymbol{b}^{\dagger}_{\lambda S}\cdot\boldsymbol{b}_{\lambda S}\\ &+(\boldsymbol{b}_{\lambda S})^2]\Big\},\end{aligned} \tag{3}$$

where $(\boldsymbol{b}^{\dagger}_{\lambda S})^2=(\boldsymbol{b}^{\dagger}_{\lambda S}\cdot\boldsymbol{b}^{\dagger}_{\lambda S})$ is a shorthand notation for the scalar product. Similarly for $(\boldsymbol{b}_{\lambda S})^2$ and $(\boldsymbol{b}^{\dagger}_{\lambda S}\cdot\boldsymbol{b}_{\lambda S})$. The factors $(1-\boldsymbol{n}_f/2\Omega)$ simulate the terms that would appear in the exact boson mapping of the quark-antiquark pairs. The $\boldsymbol{b}^{\dagger}$ and $\boldsymbol{b}$ are boson creation and annihilation operators of the gluon pairs with spin $S=0$ and color $\lambda=0$. The interaction describes scattering and vacuum fluctuation terms of fermion and gluon pairs. The strength $V_{\lambda S}$ is the same for each allowed value of λ and S, due to symmetry reasons, as shown in (I). The matrix elements of the Hamilton operator are calculated in a seniority basis. The interaction does not contain terms that distinguish between states of different hypercharge and isospin. It does not contain flavor mixing terms, either. The procedure used to adjust the four parameters (values of $V_{\lambda S}$) was discussed in detail in (I).

The disadvantage posed by working in the boson space is the appearance of unphysical states. In (I) we have presented a method that is very efficient in eliminating spurious states, as we shall show in this paper. The suitability of Hamiltonian (3) to describe the gluon pair and quark-antiquark pair contents of mesons has been discussed in detail in (I).

As a next step, in this paper, we have introduced temperature and discussed the transition to and from the QGP. As can be expected, because of the schematic nature of the model, we may attempt to describe only the general trends of the observables. To achieve this goal, further assumptions have to be made with respect to the volume of the system because the model, as has been proposed in (I), has no *a priori* information about the volume of the particle.

III. THE PARTITION FUNCTION, SOME STATE VARIABLES, AND OBSERVABLES

The group classification of basis (1) allows for a complete bookkeeping of all possible states belonging to the Hilbert space of Eq. (3). The corresponding partition function, which contains the contribution of the quark-antiquark and gluon pair configurations introduced in the preceding section, is given by

$$\begin{aligned}Z_{qg_0^2}=&\sum_{[h]}\dim(\lambda_C,\mu_C)\sum_{(\lambda_f,\mu_f)}\sum_{J}(2J+1)\\ &\times\sum_{P=\pm}\sum_{i}\mathrm{mult}(E_i)e^{-\beta(E_i-\mu_B B-\mu_s s-\mu_I I_z)},\end{aligned} \tag{4}$$

where μ_B, μ_s, and μ_I are the baryon, strange, and isospin chemical potentials, respectively. The sum over $[h]=[h_1h_2h_3]$ denotes all color irreps of U(3) with $\Sigma_k h_k=N$, where N is the total number of quarks in the two levels (Dirac's picture). The transposed Young diagram $[h]^t$, obtained by interchanging rows and columns, denotes the U(12) irrep. The index "i" refers to all states with the same color, flavor, spin, and parity (P). These states are obtained after the diagonalization of Hamiltonian (3). For mesons belonging to the π-η and ω-ρ octet, the mass values entering in Eq. (4) do not take into account flavor mixing. The eigenvalues E_i are denoted by the eigenvalue index i, and they are functions of all the numbers needed to specify the allowed configurations, namely, s, (λ_f,μ_f), P, S, $[h]$, and of the cutoff for the different boson species $[\lambda,S]$ [see (I)]. The quantities B and I_z are the baryon number and the third component of the isospin. According to the experimental evidences the value $\mu_I=0$ is a reasonable approximation, and we have consistently adopted it in our calculations. The dimension corresponding to color configurations is given by $\mathrm{mult}(\lambda_f,\mu_f)=\frac{1}{2}(\lambda_f+1)(\mu_f+1)(\lambda_f+\mu_f+2)$ and of the spin by $(2J+1)$.

Since the eigenstates of Hamiltonian (3) have been calculated after performing a boson mapping, as described in (I), we have consistently fixed the corresponding cutoff values at 2Ω, Ω, $2\Omega/3$, and $\Omega/3$ for the boson pair species [0,0], [0,1], [1,0], and [1,1], respectively [see (I)]. These values are adequate when the fermion (quark-antiquark) configurations entering in the boson states correspond to a full occupation of the fermion lower state $(-\omega_f)$. These numbers may be modified when the fermion configurations correspond to states where the upper level is partially occupied and the lower level is partially unoccupied. The distribution of the occupation in the upper and lower fermion levels is fixed for a lowest weight state $|lw\rangle$ of a given U(12) irrep, defined by $B_{\lambda f,SM}|lw\rangle=0$. The irrep of U(12) is given by a Young diagram [14] with m_k boxes in the kth row. The lowest weight state is given by $\Sigma_{k=1}^{6}m_k$ quarks in the lower level and $\Sigma_{k=7}^{12}m_k$ quarks in the upper level. The highest weight state is obtained by interchanging the occupation. The difference of the number of quarks in the upper level, appearing in the highest and lowest weight states, gives the maximal number of quarks we can excite for a given U(12) irrep. This number is given by

$$2J=\sum_{k=1}^{6}m_k-\sum_{k=7}^{12}m_k. \tag{5}$$

For the case $[3^60^6]$, used in (I), we found $J=\Omega$. Therefore, $2J$ is the maximal number of quarks we can shift to the higher level, i.e., it is equal to the maximal number of quark-antiquark pairs that can be put on top of the lowest weight state of a given U(12) irrep, which is also the state with the lowest energy in absence of interactions.

The total partition function is given by

$$Z=Z_{qg_0^2}Z_g, \tag{6}$$

where Z_g is the contribution of all gluon states [7], which does not include contributions of gluon pairs with spin zero. It is written $Z_g=\Sigma_\alpha\exp(-\beta E_\alpha)$. The values E_α can be deduced by using Eq. (40) of Ref. [7]. Except for the gluon pairs with spin zero, all other gluon states are treated as spectators because the Hamiltonian in Eq. (3) does not contain interactions with these other states. Note, that the interaction between the gluons is taken into account explicitly in the model of Ref. [7]. As a shorthand notation we will abbreviate the partition function by $Z=\Sigma_i e^{-\beta\mathcal{E}_i}$, taking into account that $\mathcal{E}_i$ contains the information about the chemical potential, and the contributions of the quarks and gluons.

The observables $\langle\boldsymbol{O}\rangle$ are calculated via [19]

$$\langle\boldsymbol{O}\rangle=\frac{\sum_i \boldsymbol{O}e^{-\beta\mathcal{E}_i}}{Z_a}, \tag{7}$$

where the index a denotes the color configurations, i.e; $a=(0,0)$ when only color zero states are considered and $a=c$ when also states with definite color are allowed. This distinction is needed to investigate the phase where color confinement is effective and the phase where color is allowed over a wide area of space. The quantities to calculate are the internal energy ($\langle E\rangle$), heat capacity ($\langle C\rangle$), average baryon number ($\langle B\rangle$), strangeness ($\langle s\rangle$), and the expectation value of different particle species ($\langle n_k\rangle$), where k refers to the quantum numbers of a particular particle and $\Sigma_k\langle n_k\rangle=1$, with the sum over all possible quantum numbers.

The particle expectation values have a simple expression because they select one of the eigenvalues at the time, thus if the state of a given particle is denoted by "i" and E_i is its energy, the particle expectation value is given by

$$\langle n_i\rangle=\frac{e^{-\beta(E_i-\mu_B B-\mu_s s)}}{Z_a} \tag{8}$$

(where we have used the value $\mu_I=0$, for the isospin chemical potential).

At this point we have to make an assumption upon the volume considered. The whole reaction volume can be divided in elementary volumes, and we assume that the elementary volume (V_{el}) is of the size of a hadron, corresponding to a sphere with a radius of the order of 1 fm. Later on we shall show that this choice is reasonable, as seen from the calculated thermodynamic properties of the whole system. Another assumption is related to the interaction, which does not take into account confinement. We shall discuss two scenarios, namely: (a) no additional interaction related to color is taken into account for temperatures above a critical (deconfinement) value, and (b) confinement is operative for temperatures below the critical deconfinement temperature. In the regime (a) the lowest state with color (1,0) lies at the energy $2\omega_f$, and it corresponds to putting one quark in the upper fermion level. Although it is a possible configuration, Hamiltonian (3) cannot act upon it. This is consistent with the fact that above a certain temperature, T_c (deconfinement temperature), only color nonsinglet states are allowed. The actual value of T_c will then give us an idea about the regime

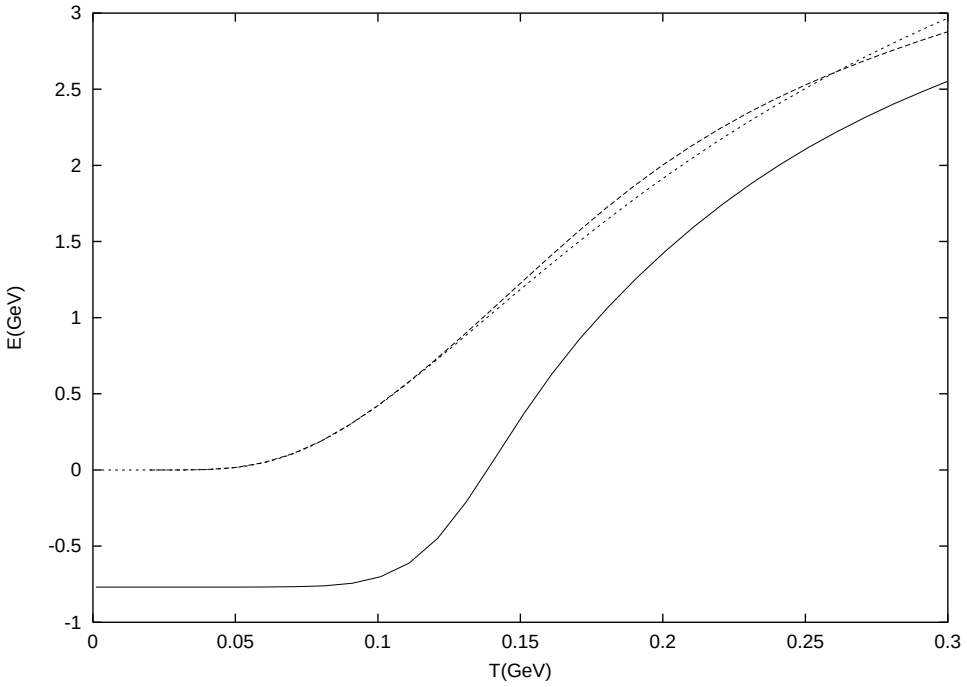

FIG. 1. Internal energy as a function of T. The dashed line corresponds to the exact result in the fermion space, without interaction. The dotted line is the internal energy calculated in the boson space with the cutoff for the different boson species, as discussed in the text. The solid line represents the results obtained with the full Hamiltonian and calculated in the boson space. No additional color interaction is taken into account.

where hadronization is operative. In the real world hadronization, i.e., confinement, should set in below a critical temperature, as a true phase transition. In our model this will be signaled by a sharp transition from a state where color nonsinglet states are still allowed ($T>T_c$) and a state where confinement is effective ($T\leqslant T_c$).

IV. DESCRIPTION OF THE HIGH TEMPERATURE REGIME: THE QGP

We shall first discuss the case where no additional color interaction is taken into account. The states with energy E_i for a given flavor, spin, and parity are obtained from the diagonalization of the model Hamiltonian, now including flavor mixing and the corrections due to the Gel'man-Okubo mass formula for the two lowest meson nonets (one with spin zero and the other with spin 1). In Fig. 1 we show the internal energy as a function of the temperature T, with and without interactions. The results shown by a dashed line have been obtained by calculating the internal energy in the fermion space *without* interactions. In this case the Hamiltonian has a simple image in the fermion space and the calculation of the partition function can be performed exactly. The dotted line shows the results obtained by working with the boson mapping, and by enforcing the corresponding cutoffs in the maximal number of bosons, as explained above and in (I). The internal energy is a good indicator of the number of active states in the Hilbert space. Note that the results shown by both curves, the dotted and dashed lines, practically coincide. This suggests that the number of active states is nearly the same in the boson and fermion spaces for a wide range of temperatures. This does not imply that all unphysical states have disappeared, but rather that the approximate method of cutting unphysical states works reasonably well. The curve shown by a solid line, in the same Fig. 1, gives the internal energy obtained from the calculation performed in the boson space and in the presence of interactions. Although the curve does not show a clear phase transition of first order (e.g., a sharp increase of the energy in a narrow interval around T_c) the behavior around $T_c=0.170$ GeV is pretty suggestive of it. We have interpreted the observed smearing-out of the curve as follows: for $T=0$ the vacuum state is dominated by pairs of the type [1,0] and in this channel a

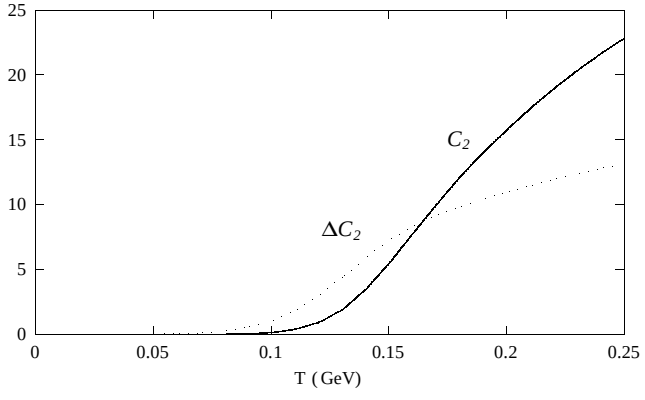

FIG. 2. The expectation value of color ($C_2=\langle \boldsymbol{C}_2\rangle$, solid line) and its variation ($\Delta C_2=\sqrt{\langle \boldsymbol{C}_2^2\rangle-\langle \boldsymbol{C}_2\rangle^2}$, dotted line) as a function of T. The variation reaches the same value as the expectation value around $T=0.170$ GeV. The values $\mu_B=\mu_s=0$ were used in the calculations.

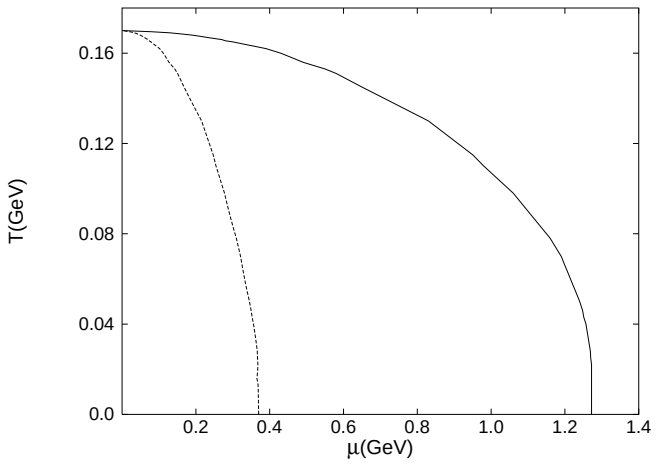

FIG. 3. Temperature versus chemical potential. The curve gives the boundary where the pressure of the system in an elementary volume of radius $r=1$ fm is equal to the bag pressure. The values of the temperature T are given as a function of the chemical potentials μ_B (solid line) and μ_s (dashed line). The label μ denotes both μ_B and μ_s.

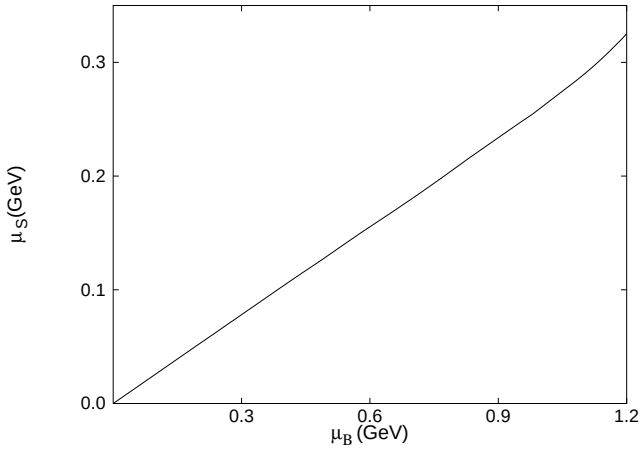

FIG. 4. Chemical potential μ_s as a function of the chemical potential μ_B, for zero local strangeness $\langle s\rangle=0$. To each pair of values (μ_B and μ_s) there corresponds a temperature T, which is determined from the limiting values shown in Fig. 3.

quantum phase transition [8] does indeed take place. By this we mean that the pairs [1,0] are effectively blocked at high temperature. The other channels contribute less significantly to the ground state [see (I)] and interact weakly than the ([1,0]) channels, therefore, they remain in a perturbative regime. Thus, as the temperature increases, an approximate first order phase transition takes place in the channel [1,0], a mechanism similar to the one shown in Ref. [8] for the [0,0] channel, while the other configurations remain unaffected. The superposition of these two mechanisms leads to the smearing out of the curve around T_c, as shown in Fig. 1.

In Fig. 2 the expectation value of the Casimir operator ($C_2=\langle \boldsymbol{C}_2\rangle$) of color and its variation ($\Delta C_2 = \sqrt{\langle \boldsymbol{C}_2^2\rangle-\langle \boldsymbol{C}_2\rangle^2}$) are shown. The eigenvalue of the Casimir operator, for an irrep with color numbers (λ_C,μ_C), is given by $C_2(\lambda_C,\mu_C)=\lambda_C^2+\lambda_C\mu_C+\mu_C^2+3(\lambda_C+\mu_C)$. As a reference, for a color (1,0) irrep $C_2=3$, while the irrep (1,1) has $C_2=9$. We assume that μ_B and μ_s are zero. It is interesting to observe that, in the present model, the variation of the color is approximately symmetric around $T=0.170$ GeV. A possible interpretation is the following: at high energy the probability to have a color nonsinglet state is large (the variation is not large enough to allow color singlet states) and a QGP is formed where color is effective over a wide range in space. From $T=0.170$ GeV on, the probability to find a state in color (0,0) is significantly increased, since the variation is large enough to allow color singlet states. In lowering the temperature the variation is much larger than the average color and the whole QGP dissolves in droplets of color zero. Within the present model, these results, of the average color and its variation, are signals of the transition to the hadronic phase. Accordingly, we assume that it takes place near $T_c=0.170$ GeV, for $\mu_B=\mu_s=0$. We may now calculate the bag pressure and construct the $T-\mu_B$ diagram. At $T=0.170$ GeV the pressure is determined via the expression $p=T\ln(Z)/V_{el}$, where $\Phi=-T\ln(Z)$ is the grand canonical partition function [19] and V_{el} is the elementary volume $V_{el}=4\pi/3r_{el}$. For $r_{el}=1$ fm we obtain a bag pressure $p^{1/4}$ of about 0.17 GeV, which is in reasonable agreement with standard values. When the chemical potentials μ_B and μ_s are different from zero, the temperature dependence of the internal energy changes and also changes the value of the temperature for which the pressure is equal to the bag pressure $p^{1/4}=0.18$ GeV. The results are shown in Fig. 3. Assuming that the local strangeness is $\langle s\rangle=0$, we arrived at a functional relation between T, μ_B, and μ_s, i.e., $f(T,\mu_B,\mu_s)=0$, which fixes μ_s as a function of μ_B. The results of this functional relation are displayed in Fig. 4. Once the chemical potential μ_s is adjusted, by using the results shown in Figs. 3 and 4, the chemical potential μ_B and the transition temperature T_c can be consistently determined.

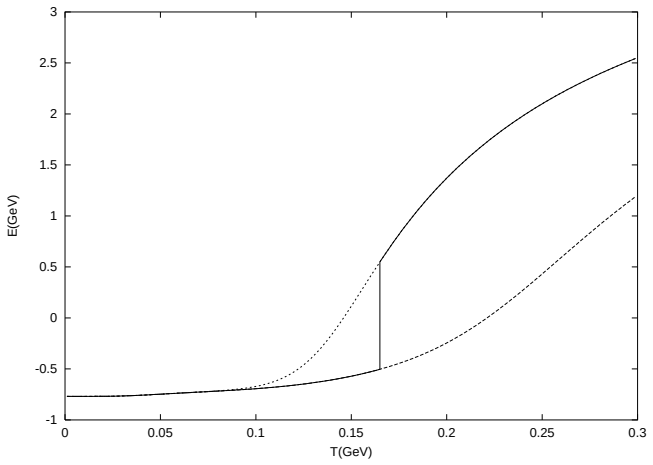

FIG. 5. Internal energy. The upper curve shows the results obtained without considering confinement. The lower curve corresponds to the results obtained with the inclusion of confinement. The solid line shows the results obtained with the partition function where confinement is considered to be fully operative below T_c ($\mu_B=\mu_s=0$).

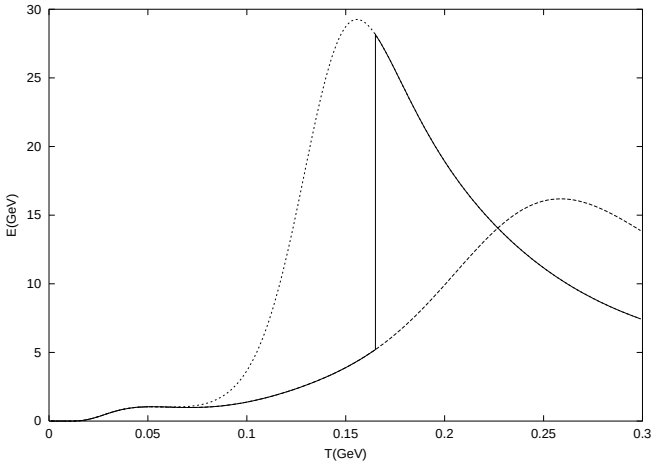

FIG. 6. Heat capacity of the system. The solid line interpolates between the case with confinement below T_c and the case without it above T_c ($\mu_B=\mu_s=0$). The dotted and dashed lines correspond, respectively, to the case where color is allowed and the one without color.

Up to now we did not take into account an interaction that generates confinement. This has to be done by hand. One possibility is to *assume* that the transition from the QGP to the hadronic phase takes place within a very small range of temperatures around the critical temperature T_c. We require that the partition function above T_c allows any color while for $T<T_c$ it contains only color zero states. Finally, chemical equilibrium connecting both phases, the QGP and the hadron gas, is understood. Figure 5 shows the results of the internal energy, without confinement (upper curve) and with confinement (lower curve). The solid line connecting both curves indicates the values for which confinement vanishes above T_c. As seen from the results, the transition is now of first order. Figure 6 shows the heat capacity calculated for the case without confinement (dotted line) and with confinement below T_c (dashed line). The solid line interpolates between them, as in the case of the internal energy (see Fig. 5).

The model can first be tested in the energy region below the transition temperature T_c, where the hadron gas should prevail. The confinement is effective and therefore we have to use the partition function $Z_{a=(0,0)}$ in Eqs. (7) and (8). We take, as an example, the measured total production rates of π^+ at 10 GeV/nucleon, as reported in the SIS-GSI experiment [20]. The system considered was Au+Au and we assume that all particles participate, i.e., $N_{part}=394$. In Fig. 2.3 of Ref. [20] a temperature of about $T=0.13$ GeV is reported. Assuming local strangeness conservation, $\langle s\rangle=0$, we obtain a relation of μ_s versus T, which is depicted in Fig. 7. From there we obtain, for the reported temperature, $\mu_s \approx 0.128$ GeV and via Fig. 4 a value $\mu_B \approx 0.55$ GeV. In Fig. 8 we show for a fixed value of μ_B, physically acceptable at temperatures near $T=0.13$ GeV, the resulting total production rate of π^+ (N_π) as a function of the temperature T. For $T=0.13$ GeV the production rate is approximately 180 pions π^+, which is close to the value of 160 obtained by using Fig. 2.3 of Ref. [20]. The good qualitative agreement with the experiment demonstrates that the present model is able, indeed, to describe, approximately, observed QCD features.

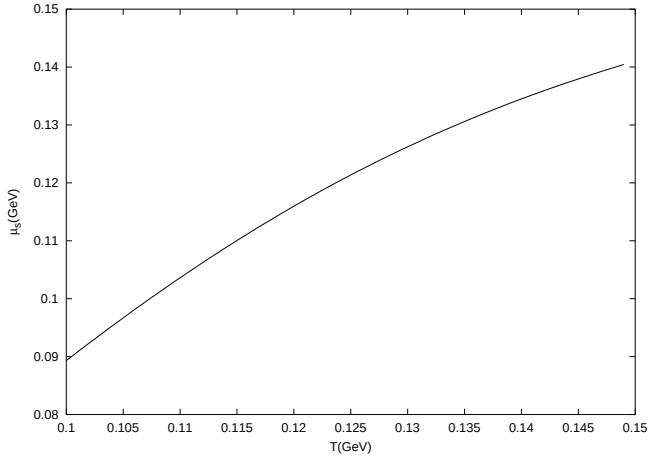

FIG. 7. The dependence of μ_s on the temperature T, for $\mu_B=0.55$ GeV and assuming $\langle s\rangle=0$, for the SIS-GSI experiment [20], Au+Au at 10 GeV/nucleon.

We have also determined ratios of particle production and some absolute production rates. The particle production is calculated for temperatures just below T_c, where only color zero states are allowed. This implies that the partition function to use is $Z_{(0,0)}$. We then apply Eq. (8). Note that in the expression of the particle-production ratios the partition function cancels out and only the dependence on the mass of the particles and the chemical potential remains. Figure 9 shows results for some particle-production ratios for beam energies $\sqrt{s}=130A$ GeV. The experimental values are taken from Ref. [21], based on the experiment described in Ref. [22] (see also Ref. [23]). For baryons, only the ratios of particle and antiparticle production are shown because these expressions are independent of the mass of the baryon. As noted in (I), the masses of the baryons are not well reproduced because they are considered as consisting of three idealized fermions on top of the meson sea. The interaction with

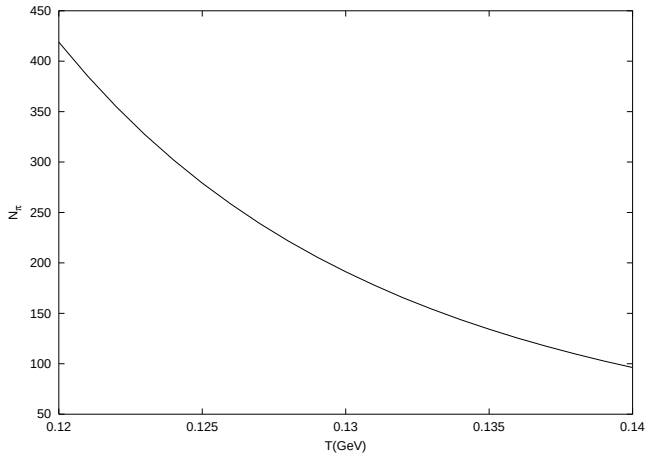

FIG. 8. Total production rate of π^+ for Au+Au at 10 GeV/nucleon [20]. For $T=0.13$ GeV the total π^+ production rate is approximately 180. The value $\mu_B=0.55$ GeV was used in the calculations, as discussed in the text.

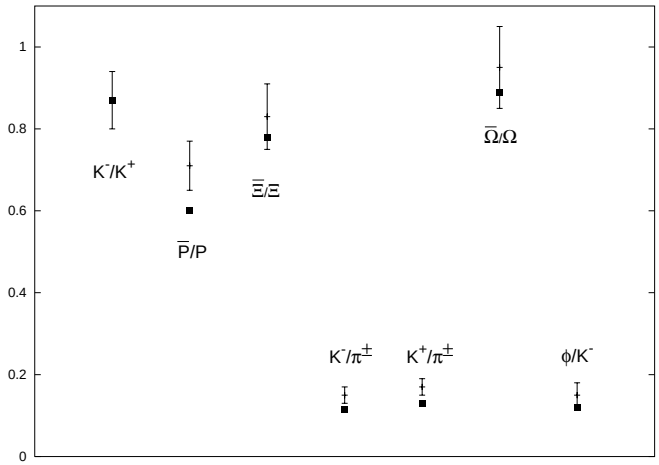

FIG. 9. Some particle-production ratios for the beam energies $\sqrt{s}=130A$ GeV taken from Ref. [21]. The calculated values are shown with full squares and the experimental values are shown within error bars.

the meson sea is not taken into account yet, but indications about how to do it are given in (I).

The central value of the K^-/K^+ production ratio, shown in Fig. 9, was reproduced with the values $\mu_s=0.012$ GeV and $\mu_B=0.044$ GeV. The other ratios are predicted by the model. Considering the simplicity of the model, the ratios are found to be in a reasonable agreement with data.

In order to obtain the total yields for kaons and for the π^+ pions it is necessary to introduce further assumptions about the size of the QGP. The baryon density is given by $\langle B\rangle/V_{el}$, where V_{el} is the size of the representative volume, as explained before. In order to conserve, on the average, the baryon number, we multiply the baryon density by the total volume and require that it must be equal to the total baryon number, given by the number of participants N_{part}. This leads to the total volume

$$V_{tot}=\frac{N_{part}V_{el}}{\langle B\rangle_a}, \tag{9}$$

where the index a refers to, as in the partition function, color ($a=c$) when the average value is calculated in the QGP and $a=(0,0)$ when it is calculated in the hadron gas. In the QGP the average value $\langle B\rangle_c$ before the transition is smaller than the average value $\langle B\rangle_{(0,0)}$ in the hadron gas after the transition. This is due to the small value of $Z_{(0,0)}$ at T_c, since many other possible color states are excluded from it which do contribute to Z_c. As a consequence, for $T=T_c$ the volume of the QGP phase, as a function of N_{part}, is much smaller than the one in the hadron gas phase. Assuming a sphere, the radius of the QGP phase is about 8 fm, and it changes to about 20 fm after the transition. This implies volumes of the order of approximately 2×10^3 fm^3 and 3.4×10^4 fm^3, respectively.

This transition is, as pointed out earlier, assumed to take place suddenly at T_c (probably it should be smeared out, but we cannot describe it with the present model). This implies that within the scenario assumed there is a rapid expansion of the volume caused by the transition from the QGP to the hadron phase, which should be observed as a large outward motion. One possible interpretation is that most of the pions are produced during the transition, liberating energy and provoking a rapid expansion of the system. The energy gained is represented by the jump between the lower and upper curves of Fig. 5, but its origin cannot be explained by the present model, where confinement was shifted by hand.

Figure 10 shows the total pion yield as a function of the temperature T, corresponding to the Au+Au collision. The upper curve describes the total yield when all nucleons par-

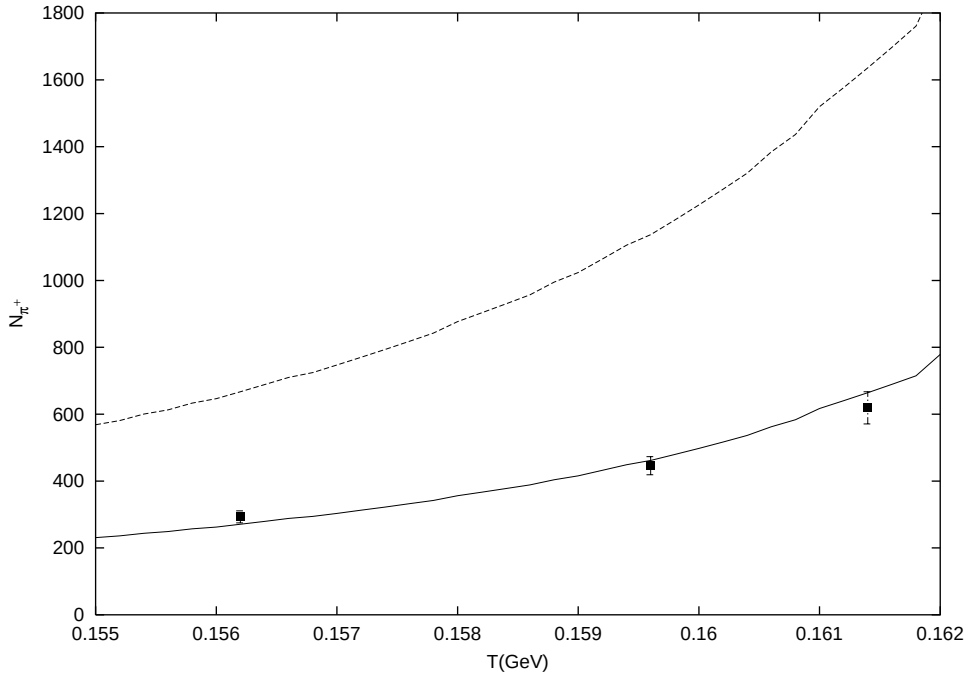

FIG. 10. Total production rate of π^+. The upper curve is for $N_{part}=394$ (Au+Au) and the lower one is for $N_{part}=250$. Data are taken from Ref. [24]. Because of $\mu_I=0$, the production rate for π^- coincides with the production rate for π^+.

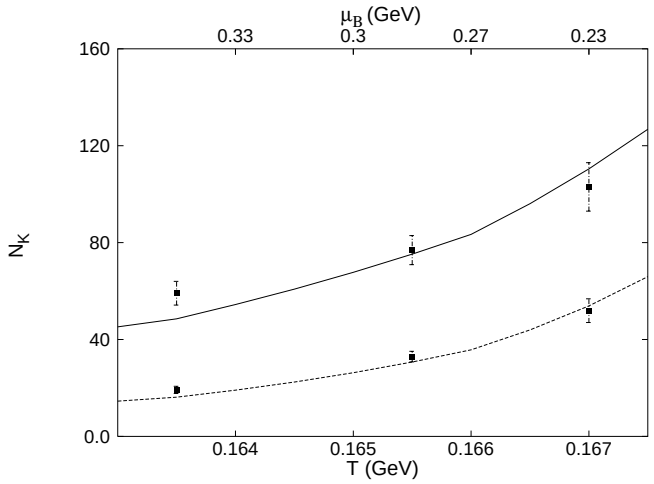

FIG. 11. Total production rate of K^+ (upper curve) and K^- (lower curve) for $N_{part}=250$. Data are taken from Ref. [24].

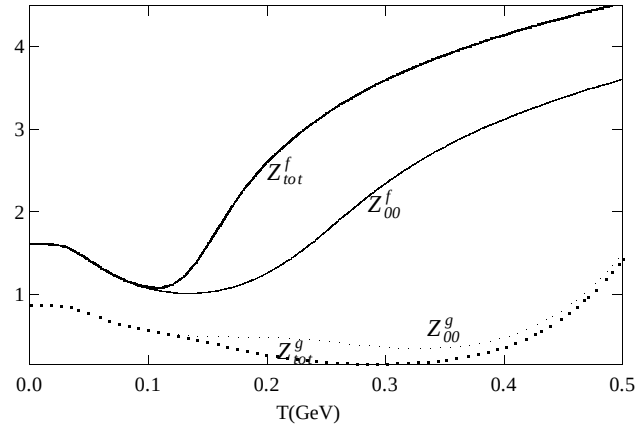

FIG. 12. Expectation value of the fermion (quark-antiquark) and gluon pairs. The symbols Z_{tot} and Z_{00}, on each curve, indicate if color was allowed. The upper indices f and g on the Z refer to fermion and gluon pairs, respectively.

ticipate, while for the lower one we have taken $N_{part}=250$. This value agrees better with the experiment, as seen from the results, and it means that in the collision about 250 nucleons participate in the QGP. In Fig. 11 the total kaon production rate is displayed. The upper curve corresponds to K^+ and the lower one to K^- absolute production rates, respectively. In both cases $N_{part}=250$ was used, the same value used previously in the calculation of the pion yield. The ratio of the curves was already adjusted at the point corresponding to the K^+/K^- ratio. The absolute production rate and the shape of the curve, however, are a prediction of the model (as far as we can talk about ''predictions'' within this toy model). Considering the simplicity of the model it is surprising that the absolute production rate is well reproduced. This feature is common to other thermodynamical descriptions of the transition from the QGP to the hadron gas [21,23].

Finally, in Fig. 12, we show the calculated expectation values of the number of quark and gluon pairs as a function of the temperature T. At $T=0$ GeV the results correspond to the fractions of gluon pairs and fermion (quark-antiquark) pairs in the physical vacuum state. At high temperatures the gluon part increases and takes over the fermion part, which shows saturation. However, at the temperatures of interest, i.e., around the point of the phase transition $T_c \approx 0.16$ GeV, the gluon number is still suppressed with respect to the fermion pair number. This might be in favor of the ALCOR model [25] which supposes a suppression of gluons in the QGP and takes only constituent quarks and antiquarks into account. Note that at $T=0.170$ GeV still a sensible amount of gluon pairs are present.

V. CONCLUSIONS

We have presented a toy model of QCD. The model is described in (I) and in this paper we have focused on the thermodynamic properties, at equilibrium, emerging from the model. We have calculated the partition function with and without color, and studied the temperature dependence of some observables, such as the internal energy, the heat capacity, and the production rates of particles. The parameters of the model were determined in (I), adjusting the meson spectrum at low energy. Without further parameters the internal energy, the heat capacity, and some particle ratios were determined, as explained in the text.

We have applied the model to the case of the Au+Au collision at 10 GeV/nucleon [20] and shown that it can reproduce qualitatively the absolute production rates of π^+. At this energy the QGP has not yet formed and, therefore, the results show that the model can be applied to study schematically the thermodynamics of a hadron gas.

Next, we have applied the model to energies where one assumes that the QGP has been already formed. The absolute production rate of π^+ and kaons were calculated, just below the transition temperature, by taking the number of participant nucleons (N_{part}) as an input. The agreement between calculated and experimental values was found to be satisfactory. Also, the resulting production rate was described reasonably well, once the μ_s chemical potential was fixed to yield the correct (observed central value) K^+/K^- ratio. Some mass-independent baryon-antibaryon ratios were qualitatively reproduced by the model predictions. This demonstrates that the model is able to describe the general trend of QCD, in the finite temperature domain, and the transition to and from the quark-gluon plasma.

ACKNOWLEDGMENTS

We acknowledge financial support through the CONACyT-CONICET agreement under the project name ''Algebraic Methods in Nuclear and Subnuclear Physics'' and from CONACyT Project No. 32729-E. S.J. acknowledges financial support from the Deutscher Akademischer Austauschdienst (DAAD) and SRE. S.L. acknowledges financial support from DGEP-UNAM. Financial help from DGAPA, Project No. IN119002, is also acknowledged.

[1] S. Lerma, S. Jesgarz, P. O. Hess, O. Civitarese, and M. Reboiro, Phys. Rev. C **67**, 055209 (2003), preceding paper.
[2] H.J. Lipkin, N. Meschkov, and S. Glick, Nucl. Phys. **A62**, 118 (1965).
[3] D. Schütte and J. Da Providencia, Nucl. Phys. **A282**, 518 (1977).
[4] S. Pittel, J.M. Arias, J. Dukelsky, and A. Frank, Phys. Rev. C **50**, 423 (1994).
[5] J. Dobes and S. Pittel, Phys. Rev. C **57**, 688 (1998).
[6] J.G. Hirsch, P.O. Hess, and O. Civitarese, Phys. Lett. B **390**, 36 (1997); O. Civitarese, P.O. Hess, and J.G. Hirsch, *ibid.* **412**, 1 (1997); J.G. Hirsch, P.O. Hess, and O. Civitarese, Phys. Rev. C **56**, 199 (1997).
[7] P.O. Hess, S. Lerma, J.C. López, C.R. Stephens, and A. Weber, Eur. Phys. J. C **9**, 121 (1999).
[8] S. Lerma, S. Jesgarz, P.O. Hess, O. Civitarese, and M. Reboiro, Phys. Rev. C **66**, 045207 (2002).
[9] A.P. Szczepaniak, E.S. Swanson, C.-R. Jia, and S.R. Cotanch, Phys. Rev. Lett. **76**, 2011 (1996); E.S. Swanson and A.P. Szczepaniak, Phys. Rev. D **56**, 5692 (1997); P. Page, E.S. Swanson, and A.P. Szczepaniak, *ibid.* **59**, 034016 (1999); E.S. Swanson and A.P. Szczepaniak, *ibid.* **59**, 014035 (1999).
[10] U. Löring, B.Ch. Metsch, and H.R. Petry, Eur. Phys. J. A **10**, 309 (2001); **10**, 395 (2001); **10**, 447 (2001).
[11] B. Müller, *The Physics of the Quark-Gluon Plasma*, Lecture Notes in Physics Vol. 225 (Springer, Heidelberg, 1985); J. Lettessier and J. Rafleski, *Hadrons and Quark-Gluon Plasma* (Cambridge University Press, Cambridge, 2002).
[12] S. A. Bass, Pramana (to be published), nucl-th/0202010, and references therein.
[13] J.P. Draayer and Y. Akiyama, J. Math. Phys. **14**, 1904 (1973); J. Escher and J.P. Draayer, *ibid.* **39**, 5123 (1998).
[14] M. Hamermesh, *Group Theory and its Application to Physical Problems* (Dover, New York, 1989).
[15] R. López, P.O. Hess, P. Rochford, and J.P. Draayer, J. Phys. A **23**, L229 (1990).
[16] S. Lerma, program for the reduction of U(12) to $SU_f(3) \otimes SU_S(2)$, UNAM, Mexico, 2002.
[17] A. Klein and E.R. Marshalek, Rev. Mod. Phys. **63**, 375 (1991).
[18] K. T. Hecht, *The Vector Coherent State Method and its Applications to Physical Problems of Higher Symmetries*, Lecture Notes in Physics Vol. 290 (Springer-Verlag, Heidelberg, 1987).
[19] W. Greiner, L. Neise, and H. Stöcker, *Thermodynamics and Statistical Mechanics* (Springer-Verlag, Heidelberg, 1994).
[20] P. Senger and H. Ströbele, J. Phys. G **25**, R59 (1999).
[21] J. Rafelski and J. Letessier, nucl-th/0209084.
[22] K. Adcox *et al.*, PHENIX Collaboration, Phys. Rev. Lett. **89**, 092302 (2002); J. Castillo *et al.*, STAR Collaboration (unpublished); K. Adcox *et al.*, PHENIX Collaboration, Phys. Rev. Lett. **88**, 242301 (2002); C. Adler, STAR Collaboration, Phys. Rev. C **65**, 041901(R) (2002).
[23] P. Braun-Munzinger, I. Heppe, and J. Stachel, Phys. Lett. B **465**, 15 (1999); P. Braun-Munzinger and J. Stachel, J. Phys. G **28**, 1971 (2002).
[24] NA49 Collaboration, nucl-ex/0205002.
[25] T.S. Biró, P. Lévai, and J. Zimányi, Phys. Lett. B **347**, 6 (1995); J. Phys. G **27**, 439 (2001); **28**, 1561 (2002).